Breakout Session 7. *Aerosol type from satellite*

Moderator: ***Thomas Popp*** *Rapporteur:* ***Hongbin Yu***

Start: EU 5:30 PM / NY 11:30 AM / CA 8:30 AM / JP 0:30 AM / CN 11:30 PM

<u>Posters (5 min each presentation, including questions)</u>

Anu Kauppi: Aerosol estimates when applied to TROPOMI

Quianqian Song: Dust Climatology derived from CALIOP and MODIS

Ying Zhang: Improved inversion of aerosol components

Jason Tackett: CALIOP Aerosol Typing Performance

Soheila Jafariserajehlou: PMAp: synergistic aerosol products from Metop

Antti Lipponen: Retrieval Post-Process Corrections

<u>Talks also to be considered in in the general discussion</u>

Hongbin Yu: African Dust Intrusion into the Caribbic

Kostas Tsigaridis: Clear-sky AOD in modelling

Tero Mielonen: Comparing aerosol types

<u>General discussion</u>

Follow-up from plenary session 9

Focus on aerosol type retrieval methods from satellite

ILMATIETEEN LAITOS
METEOROLOGISKA INSTITUTET
FINNISH METEOROLOGICAL INSTITUTE

Studying aerosol type selection and retrieved AOD estimates when applied to TROPOMI measurements

Anu Kauppi[1]

joint work with Johanna Tamminen[1] & Marko Laine[1] (Methodology) and

Antti Kukkurainen[1] & Antti Lipponen[1] (radiative transfer and aerosol expertise)

[1]Finnish Meteorological Institute, Finland

15/10/2020 The 19th AeroCom and the 8th AeroSAT workshops, October 12-16, 2020

Motivation, Background and Data

- Heritage in work with OMI/Aura data and retrieval scheme similar to the OMI multi-wavelength OMAERO algorithm
  - References
    - Kauppi, A., Kolmonen, P., Laine, M., and Tamminen, J.: Aerosol-type retrieval and uncertainty quantification from OMI data, Atmos. Meas. Tech., 2017
    - Määttä, A., Laine, M., Tamminen, J., and Veefkind, J. P.: Quantification of uncertainty in aerosol optical thickness retrieval arising from aerosol microphysical model and other sources, applied to Ozone Monitoring Instrument (OMI) measurements, Atmos. Meas. Tech., 2014.
- Bayesian inference for LUT-model selection, AOD estimate and uncertainty
- Retrieving
  - AOD estimate at 500 nm based on MAP (maximum a posterior) estimate
  - Acknowledge uncertainty due to model selection and approximations in forward modeling
  - Uncertainty expressed as posterior density function

$$R_{\mathrm{obs}}(\lambda) = R_{\mathrm{mod}}(\tau, \lambda) + \eta(\lambda) + \epsilon_{\mathrm{obs}}(\lambda)$$

Model discrepancy term

Data:
- TROPOMI/S5p L1b radiance and irradiance at wavelength bands:

Band3: 342.5, 354.0, 367.0, 376.5, 388.0, 399.5 nm
Band4: 406.0, 416.0, 425.5, 436.5, 440.0, 451.5, 463.0, 483.5, 494.5 nm
Band5: 675 nm

- Surface pressure from TROPOMI UV Aerosol Index product
- Surface reflectance from **ADAM** (A surface reflectance Database for ESA's earth observation Missions) database

MOPSMAP

libRadtran

LUTs (at this moment):
- WA 9
- BB 27
- DD 24+6

ILMATIETEEN LAITOS
METEOROLOGISKA INSTITUTET
FINNISH METEOROLOGICAL INSTITUTE

Case 1. TROPOMI/S5p Orbit 11568 6-Jan-2020

Preliminary results

Smoke drifted from Australian bushfires toward South America

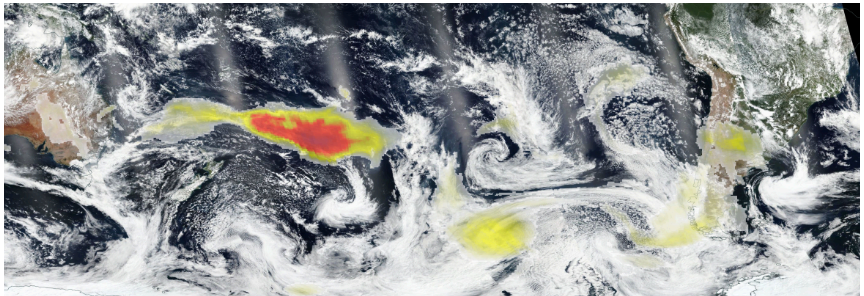

NASA Worldview: Suomi NPP/VIIRS (True color)

Data:

- TROPOMI/S5p L1b data
- Surface pressure: from TROPOMI/S5p UVAI product
- Surface reflectance: ADAM database

Pixel (262,1822)

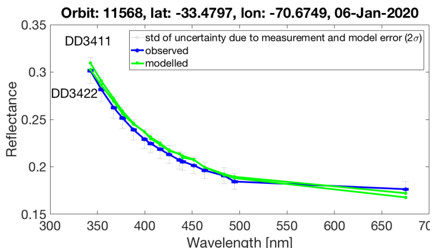

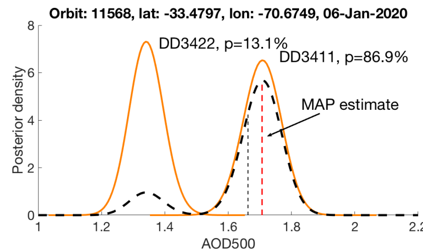

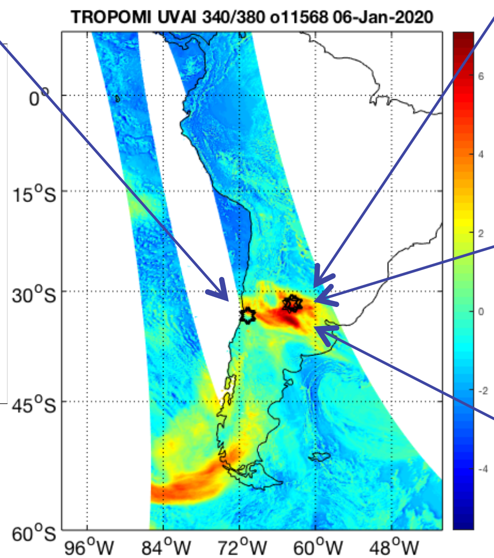

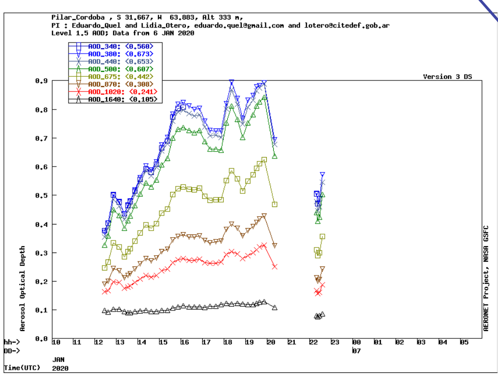

AERONET Pilar_Cordoba (31.667S, 63.883W) V3 Level 1.5 AOD

Pixel (394,1834)

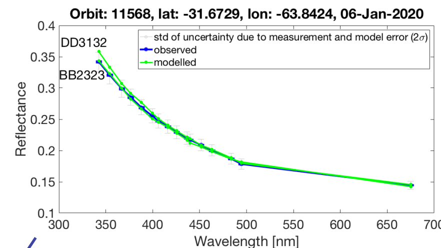

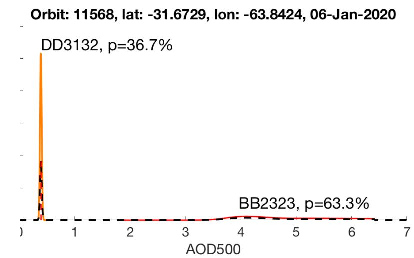

Pixel (390,1830)

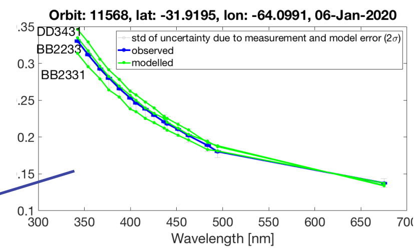

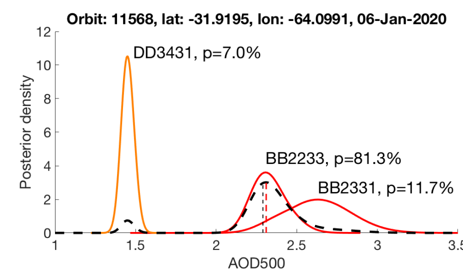

Pixel (400,1828)

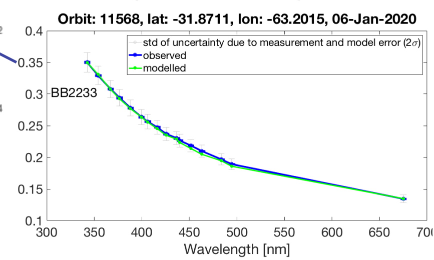

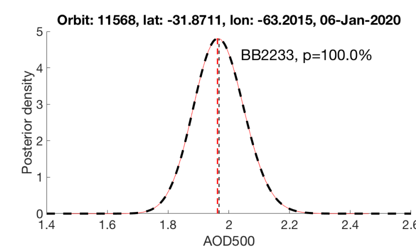

ILMATIETEEN LAITOS
METEOROLOGISKA INSTITUTET
FINNISH METEOROLOGICAL INSTITUTE

Case 2. TROPOMI/S5p Orbit 07450 22-Mar-2019

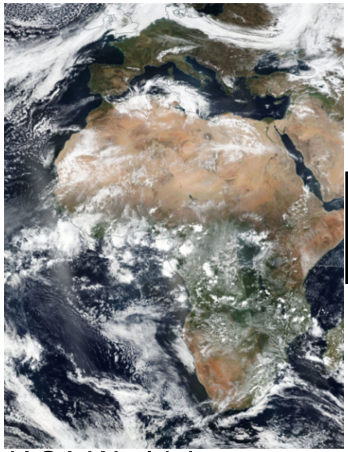

NASA Worldview:
Suomi NPP/VIIRS (True color)

Data:
- TROPOMI/S5p L1b data
- Surface pressure: from TROPOMI/S5p UVAI product
- Surface reflectance: ADAM database

Preliminary results

Model number xxxx: 1.) main type, 2.) imag. refractive index, 3.) vertical distr., 4.) size distr.

Pixel (285,2264)

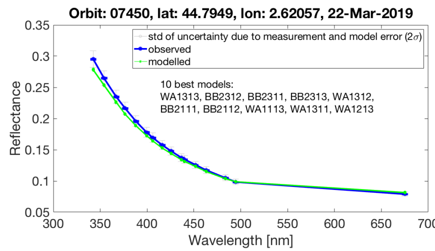

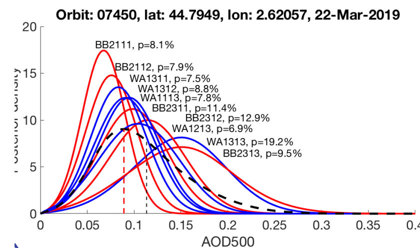

Pixel (376,1832)

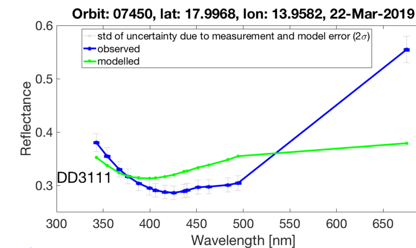

Pixel (278,1935)

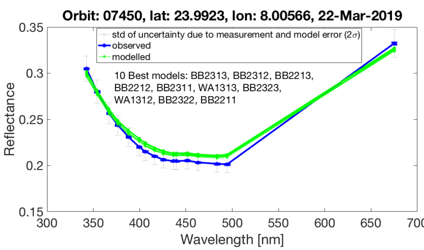

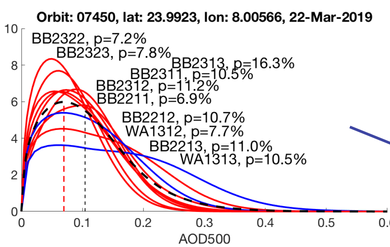

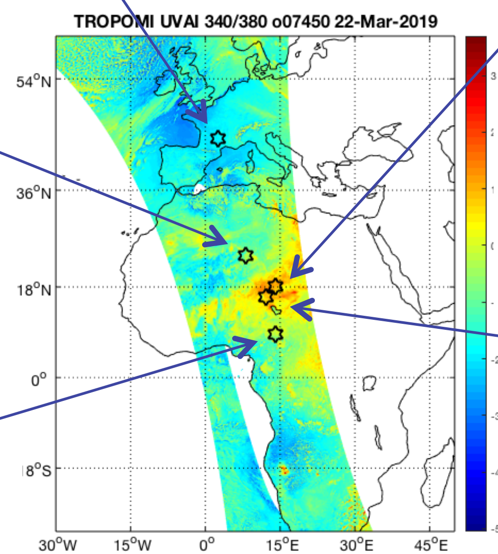

Pixel (332,1804)

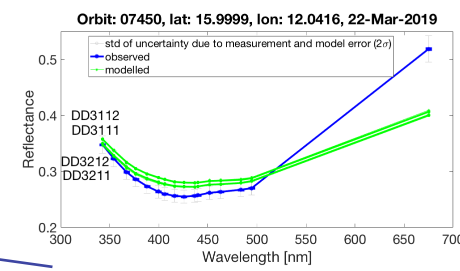

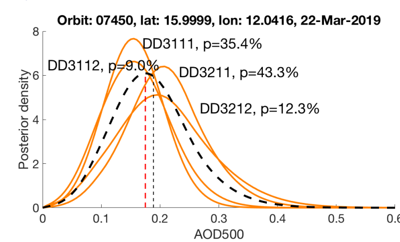

Pixel (342,1687)

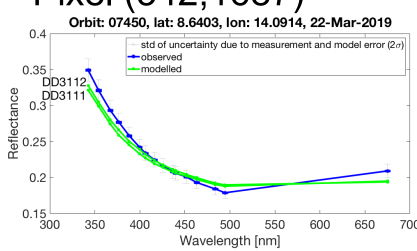

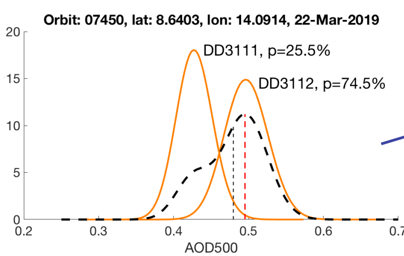

ILMATIETEEN LAITOS
METEOROLOGISKA INSTITUTET
FINNISH METEOROLOGICAL INSTITUTE

Next steps

Please note, these are preliminary results and under verification

- This work is going on, including
  - check the measurement error
  - Here was used the model discrepancy term (i.e. model error) estimate form the previous studies with OMI data. The model discrepancy term will be estimated for this study.
  - check LUTs functioning
  - examine the retrieved results and compare to e.g. AERONET data
- A lot more study cases are needed
- Paper in preparation

Acknowledgements: Academy of Finland CoEinv for funding and scientific support, we thank the AERONET PIs and site managers for providing the data, the ADAM products have been collected from the ADAM database (adam.noveltis.com) and were produced by the ADAM team under the European Space Agency (ESA) study contract Nr C4000102979.

Thank you!

Global DAOD climatology derived from CALIOP and MODIS aerosol retrievals on decadal time scales: regional and interannual variability

Qianqian Song[1,2], Zhibo Zhang[1,2], Hongbin Yu[3]

1. Physics Department, UMBC, Baltimore, Maryland, USA
2. Joint Center of Earth Systems Technology, UMBC, Baltimore, Maryland, USA
3. Goddard Space Flight Center, NASA, Greenbelt, Maryland, USA

Sensors	Retrieve Scope	Relevant variables used to derive DAOD	References
MODIS	Ocean	AOD, fine mode fraction	Kaufman et al.2005 Yu et al.2009,2020
MODIS	Land	Spectral SSA, Angstrom exponent	Ginoux et al. 2010
CALIOP	Globe	Profiles of backscatter and depolarization ratio	Yu et al.2015a

Multi-wavelength observations from MODIS contains **aerosol size** information such as fine mode fraction and Angstrom wavelength exponent in the observed reflectance spectral pattern, which was used to separate dust aerosols from others in MODIS dust retrieval over ocean and land.

CALIOP uses observations of backscatter coefficient which contains dust **shape information** to separate dust aerosols from others.

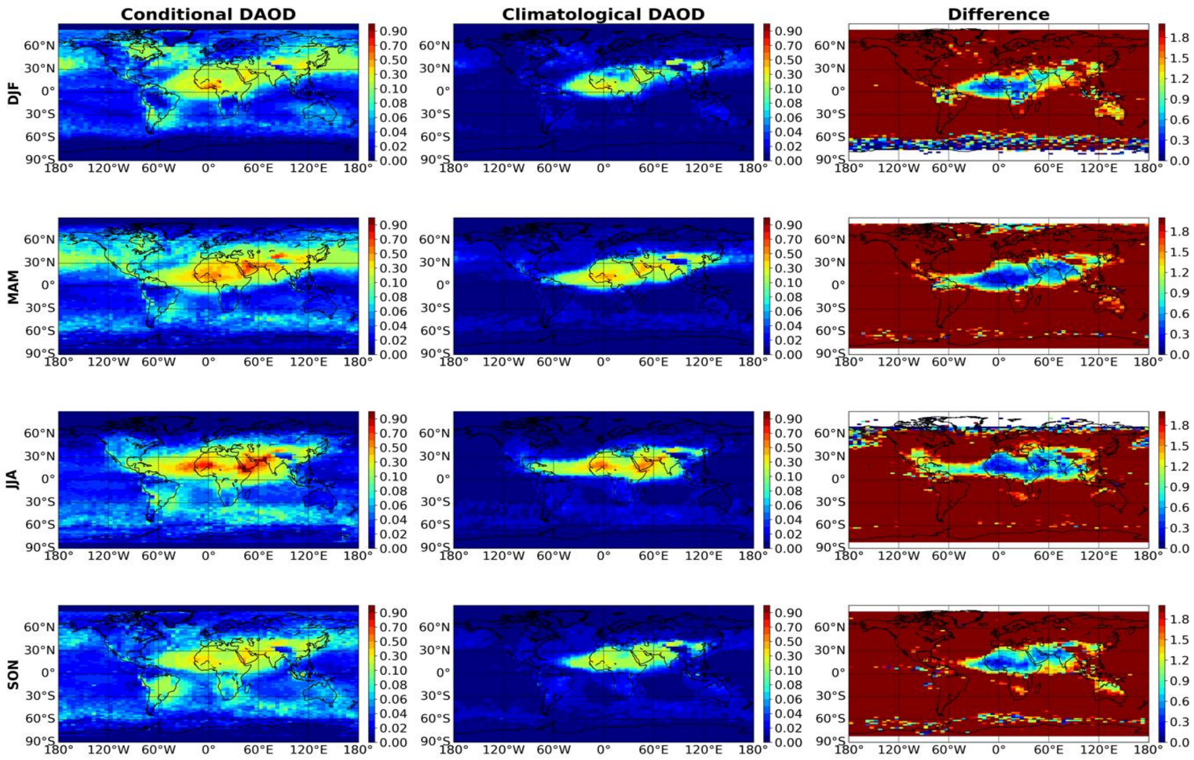

CALIOP dust climatology(2nd column) show high DAOD in 'dust belt' region, but DAOD value is rather low in some other regions known to be dusty in certain seasons. Those regions do stand out in MODIS DAOD plots (shown in slide 2).

Climatological DAOD contains both dust frequency and dust intensity information, while conditional DAOD diminishes impacts from dust frequency by excluding dust-free cases in the average. It is mainly related to dust intensity.

The low difference between conditional and climatological DAOD indicates that dust activities over there are persistent.

The large difference in other regions suggest that dust activities in those regions are highly episodic and occur in relatively small scale.

. **DAOD climatology derived from MODIS dust retrieval**

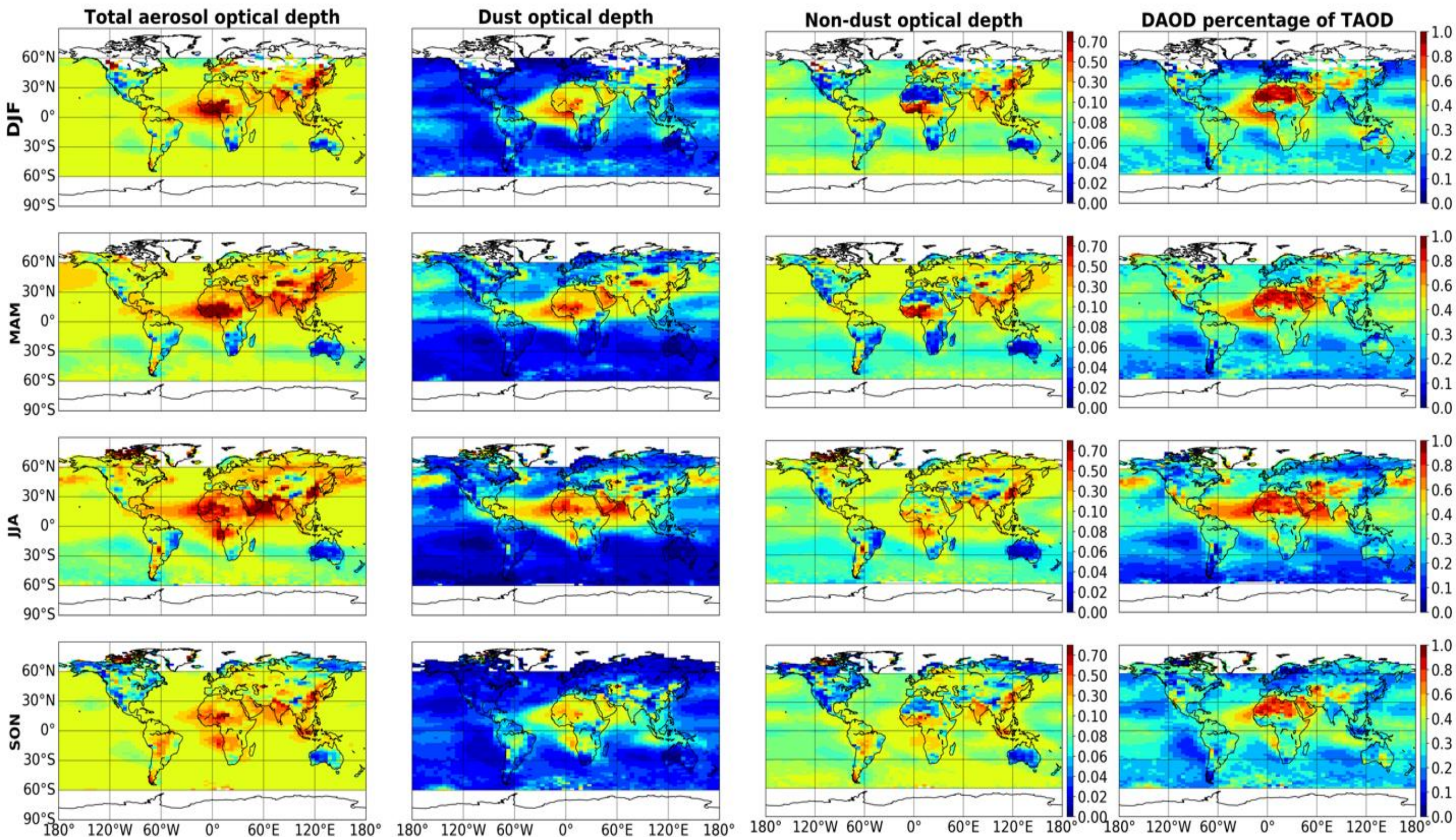

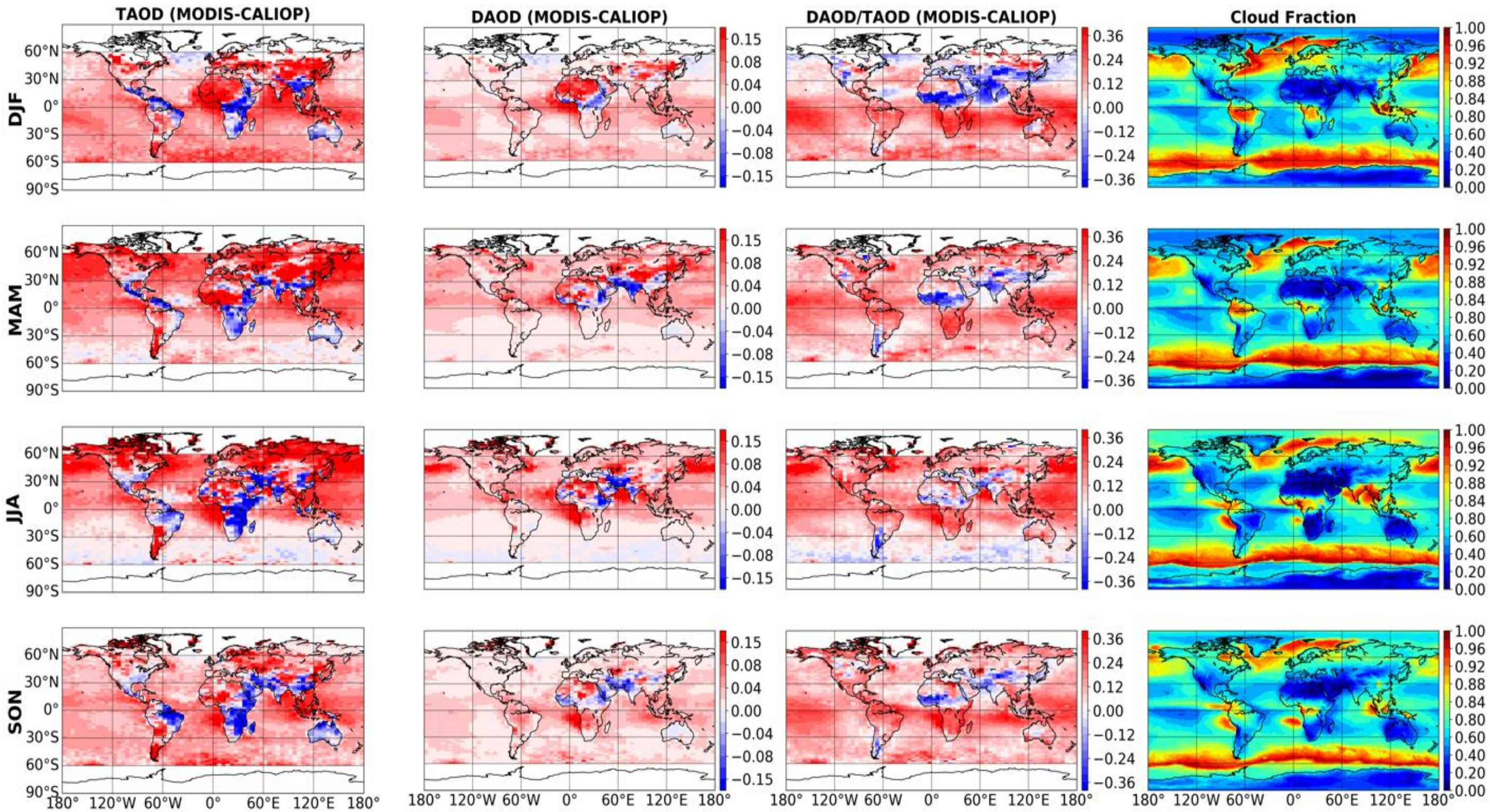

The difference between MODIS and CALIOP in 10-year (2007-2016) seasonal mean TAOD (1st column), DAOD (2nd column), the percentage of DAOD in TAOD (3rd column) and 10-year seasonal mean cloud fraction from MODIS L3 product (4th column).

MODIS DAOD is generally larger than CALIOP DAOD due to :

1. Uncertainty associated with TAOD retrieval.
2. Different dust detection and separation. CALIOP is based on dust shape, MODIS is based on dust size.

UMBC

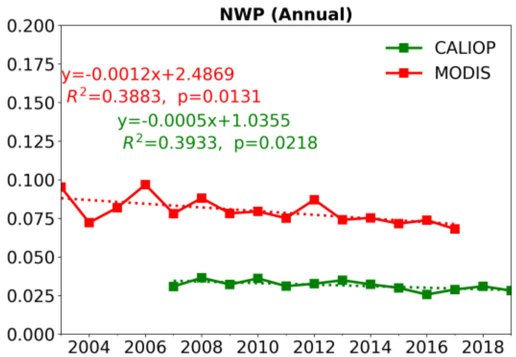

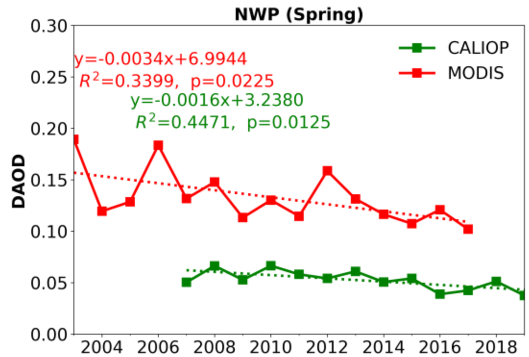

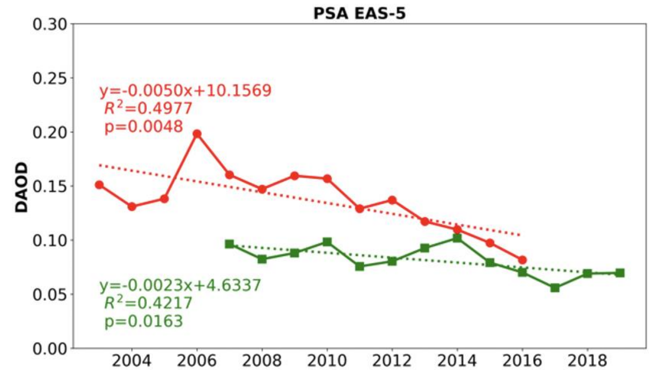

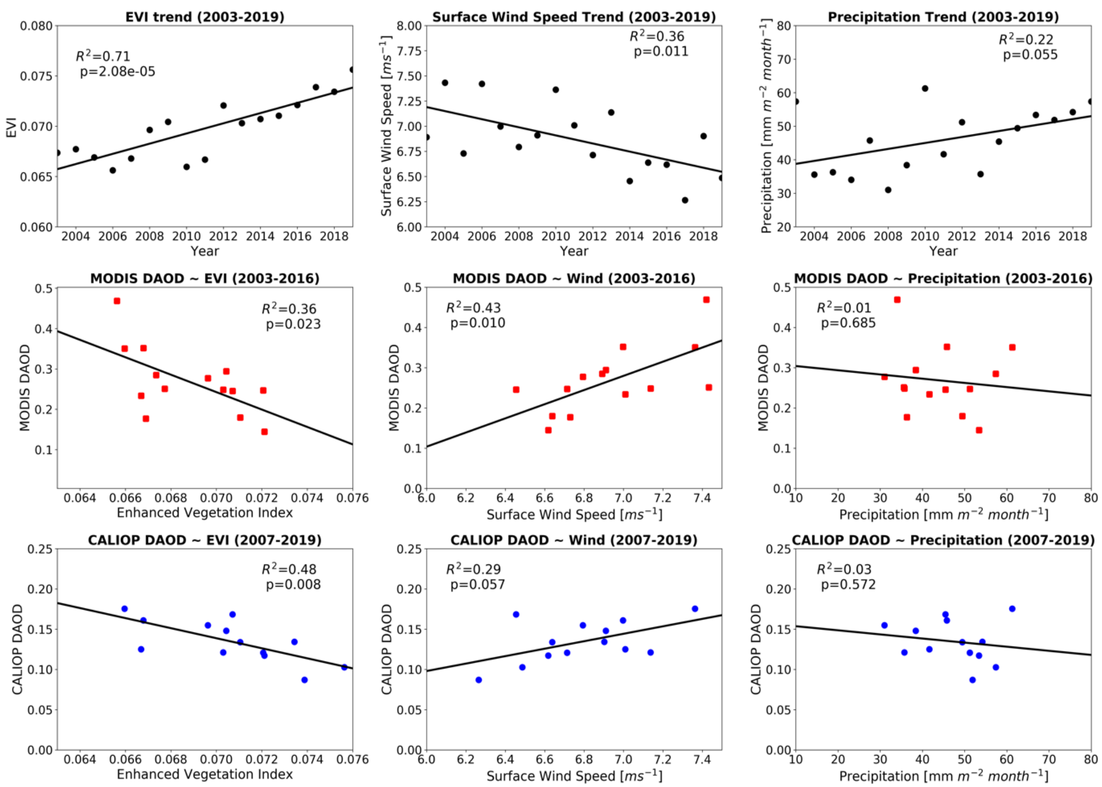

The interannual variability of DAOD over dust-laden regions show no clear trend except the NWP region with a decreasing trend of -1.5% yr^{-1} based on MODIS and CALIOP with p < 0.05.

This trend is mainly attributed to the decreasing trend in spring with a rate of 3.66%yr^{-1} based on MODIS and 2.82%yr^{-1} based on CALIOP.

Further investigation of DAOD trend in six dust source areas in Eastern Asian where NWP dust aerosols come from shows that there is an obvious decreasing trend in DAOD over Southern Gobi Desert based on both CALIOP and MODIS dust retrievals .

The decreasing trend of DAOD is correlated significantly with the vegetation index and surface wind speed in the area, whereas, there is almost no correlation with the precipitation .

Improved inversion of aerosol components in the atmospheric column from remote sensing data

Ying Zhang, Zhengqiang Li and Gerrit de Leeuw

Aerospace Information Research Institute, Chinese Academy of Sciences
Royal Netherlands Meteorological Institute (KNMI), R&D Satellite Observations

Methodology

The aerosol components in this algorithm comprise five species, combining eight sub-components including:

- black carbon (BC)
- water-soluble (WSOM), water-insoluble organic matter (WIOM)
- ammonium nitrate(AN), sodium chloride (SC)
- dust-like (DU)
- aerosol water content (AWf and AWc)

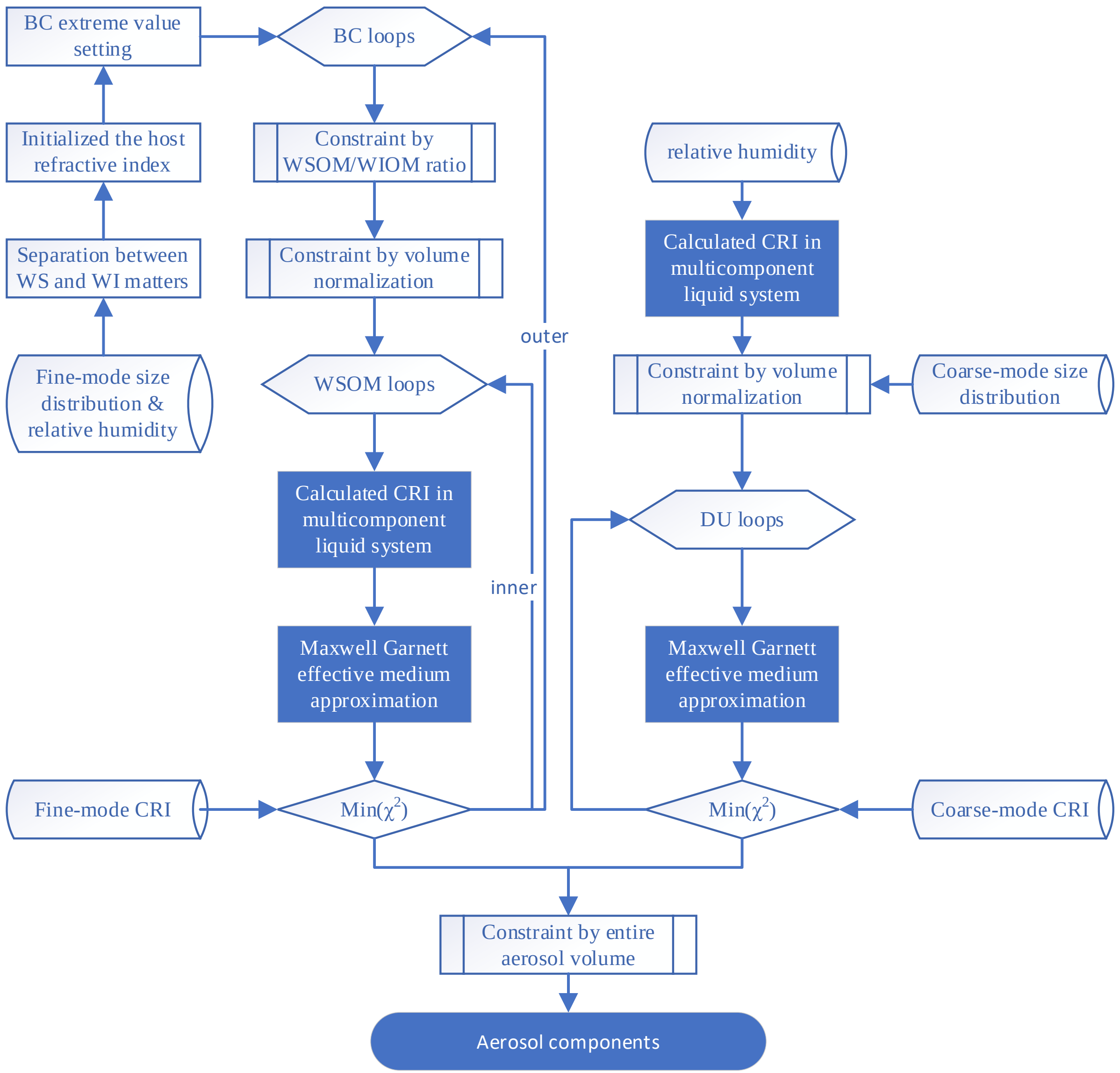

Distribution of aerosol components over China

- The atmospheric columnar DU component is dominant in the northern region of China, whereas the AW is higher in the southern coastal region.
- The SC component retrieved over the desert in northwest China originates from a paleo-marine source.
- The AN significantly decreased from 2011 to 2016, by 21.9 mg m-2, which is inseparable from China's environmental control policies.

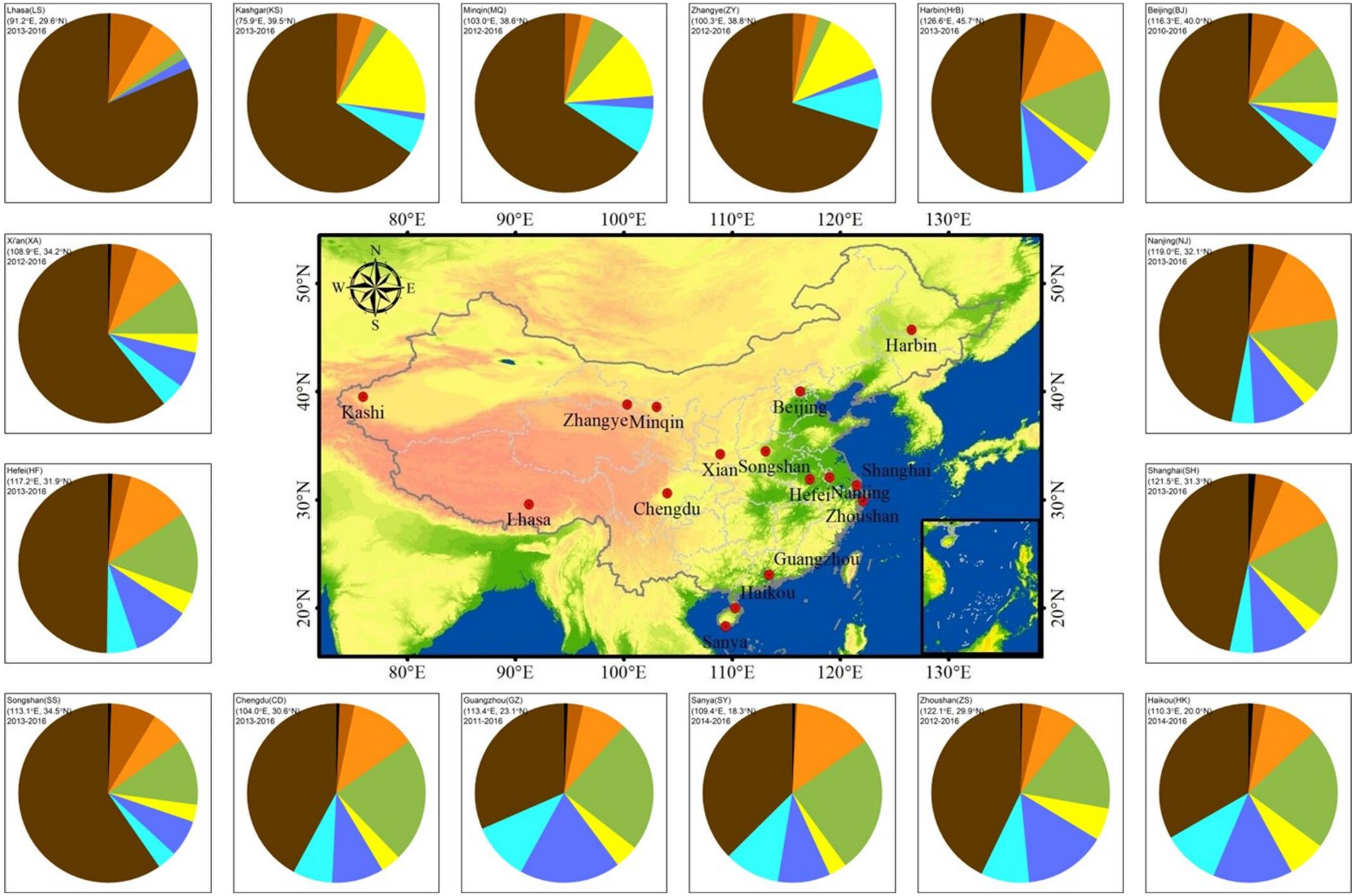

Seasonal differences over south and north China

- BC concentrations in typical northern regions are higher than in southern regions, because of emissions due to winter heating only in the north.
- The higher mass concentration of mean AN in the southern region suggests that more AN is produced by secondary reactions in the humid climate in the south than in the northern region.

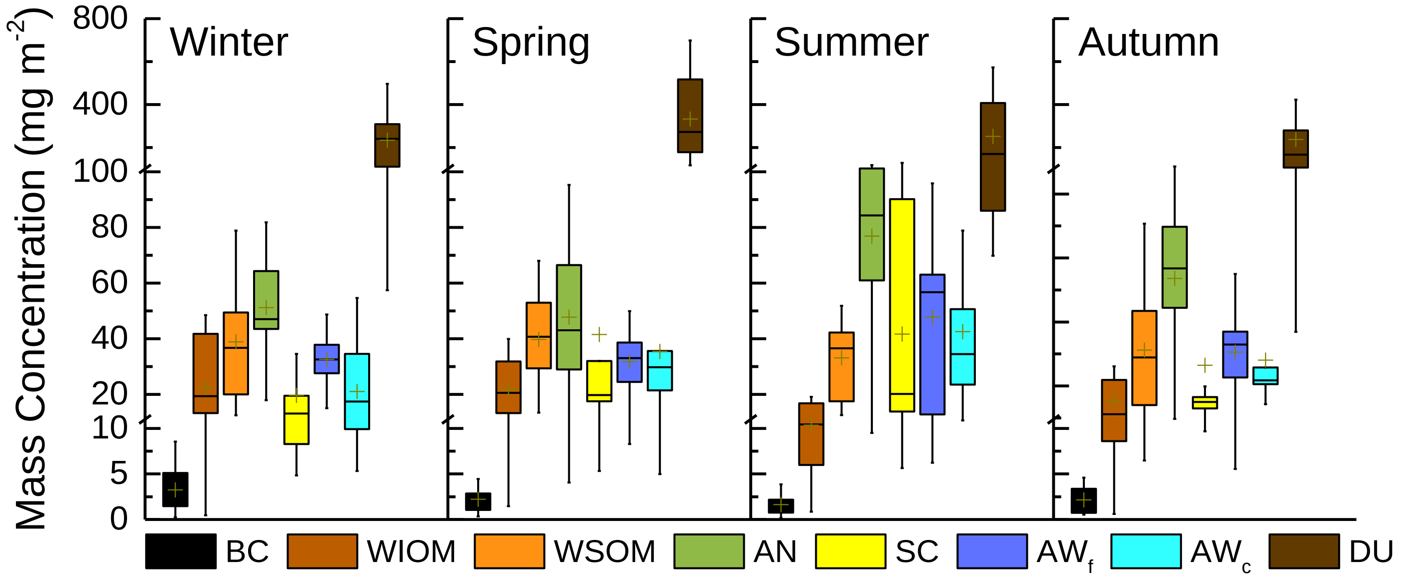

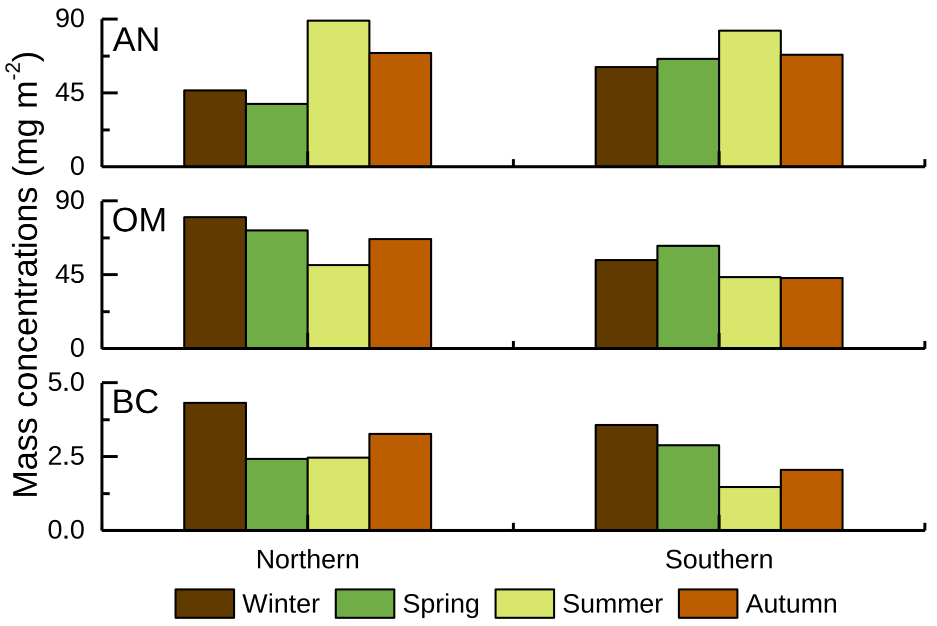

Comparison with surface observations

- OM components from the improved algorithm (2020) have good correlation with observations.
- Black carbon is closer to the identity line although the correlation coefficient is slightly smaller than that in 2018.
- For AN, the improved algorithm (2020) shows a good effect. The slope with ground observations changes from negative to positive.

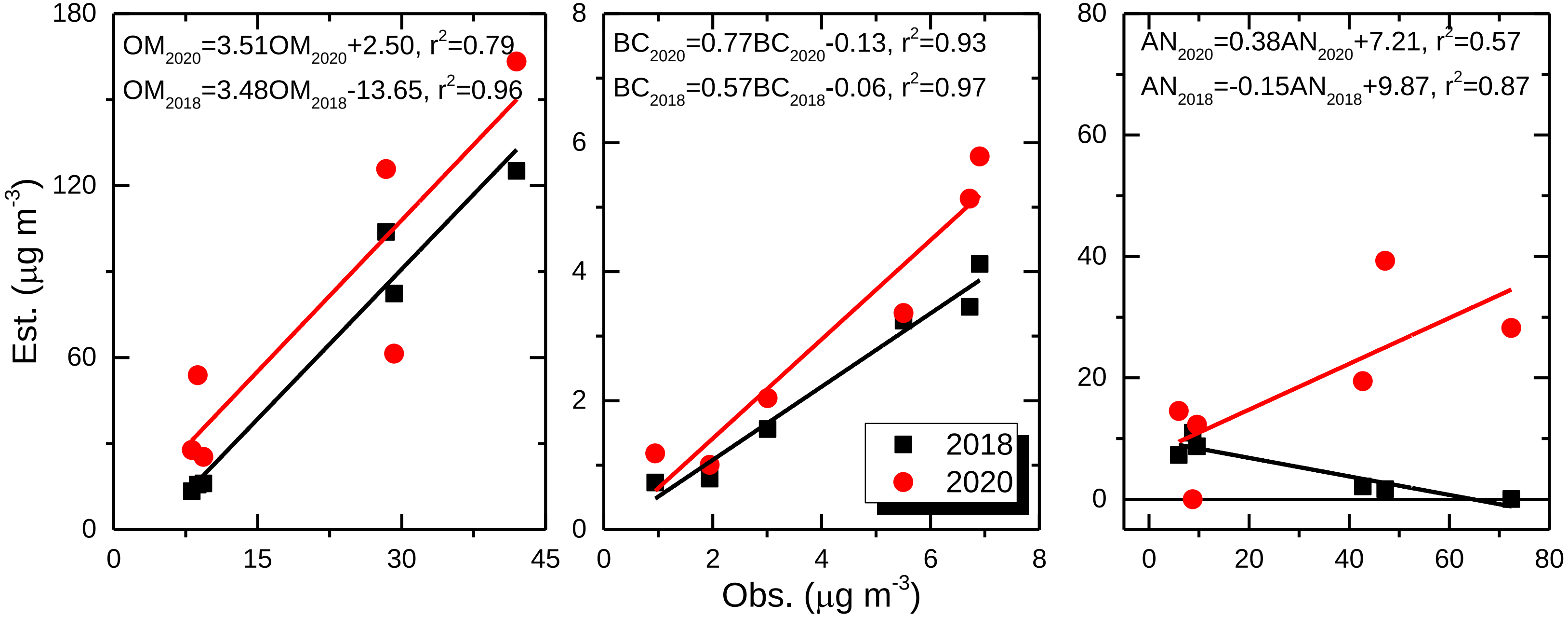

The method presented can be used not only for ground-based sun-sky photometer measurements, but also for other remote sensing instruments (e.g. Lider), and even for satellite remote sensing in the future. Meanwhile, as long as measurements of multi-wavelength extinction coefficients and aerosol size distributions are available, the inversion of aerosol composition can also be performed using surface observations. Therefore, this method can be widely used in low-cost and wide-area measurements in the future, providing a possibility for obtaining the global distribution of aerosol composition.

CALIOP Stratospheric Aerosol Typing Performance from the 2019-2020 Australian Bushfire Event

Jason Tackett[1], Jay Kar[2], Ali Omar[1], Dave Winker[1] and Mark Vaughan[1]

jason.l.tackett@nasa.gov

- CALIOP level 2 products discriminate between smoke, volcanic ash, and volcanic sulfate above the tropopause
- Upcoming revisions to the stratospheric aerosol typing algorithm in V4.5 will improve discrimination between depolarizing smoke and volcanic ash
- The pyroCb events in Australia injected a large amount of depolarizing smoke into the stratosphere.
- The current CALIOP products misclassifies 70% of these smoke layers as ash or sulfate.
- The prototype V4.5 algorithm classification is predominantly smoke (61%).

Daily CALIOP stratospheric aerosol classification below 20°S

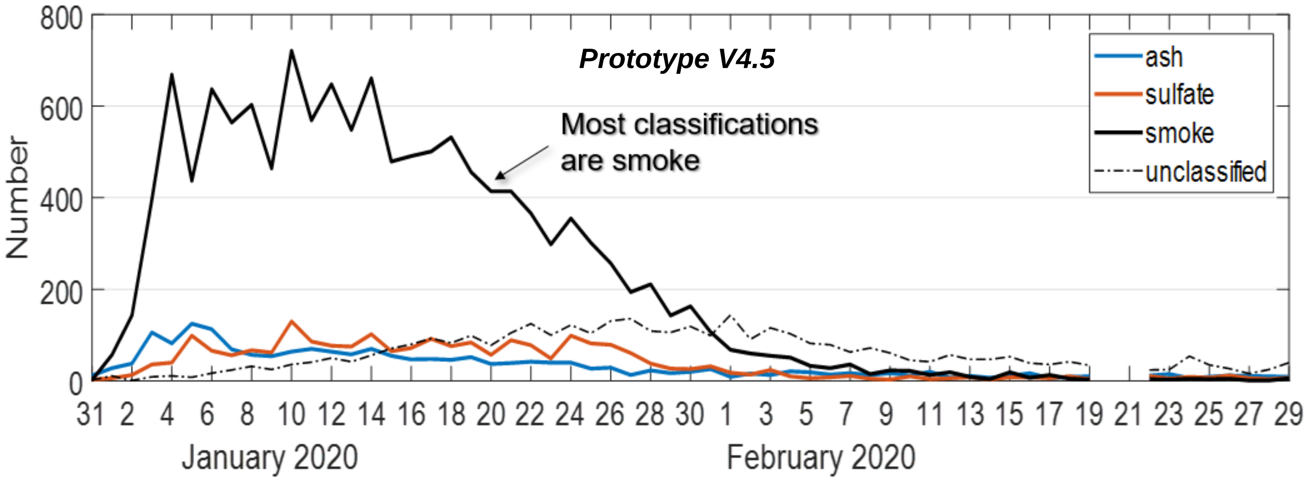

Example CALIOP Observation on 2020-Jan-03

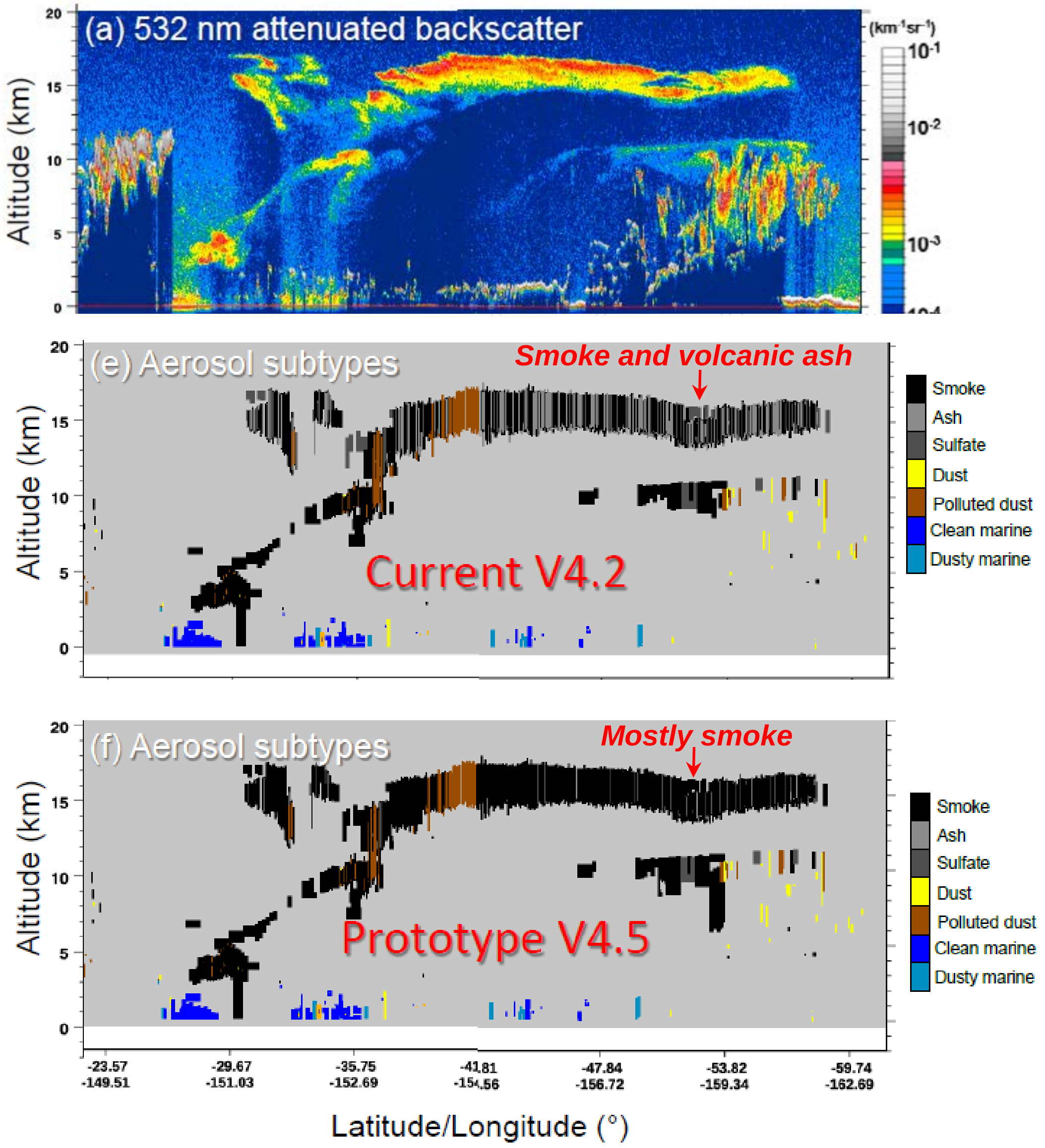

[1]NASA Langley Research Center, Hampton, Virginia; [2]Science Systems and Applications, Inc., Hampton, Virginia.

Example CALIOP Observation on 2020-Jan-03

A series of pyroCb events occurring in southeast Australia in late December 2019 and early January 2020 injected a large amount of smoke into the stratosphere. This CALIOP observation captured the smoke plume east of Australia on January 3rd at 11 UTC. The stratospheric smoke is measurably different as compared to smoke at lower altitudes. Namely, the depolarization ratio measured by CALIOP was higher.

The CALIOP cloud-aerosol discrimination algorithm classified some of this plume as stratospheric aerosol and others as ice cloud. The latter is due to the elevated color ratio and depolarization which are characteristics of ice clouds. The aerosol subtypes determined by the CALIOP level 2 algorithms are shown. Whereas the current V4.2 release classifies this plume as a mixture of smoke and volcanic ash (a misclassification), the prototype V4.5 release classifies the bulk of the plume in this example as smoke.

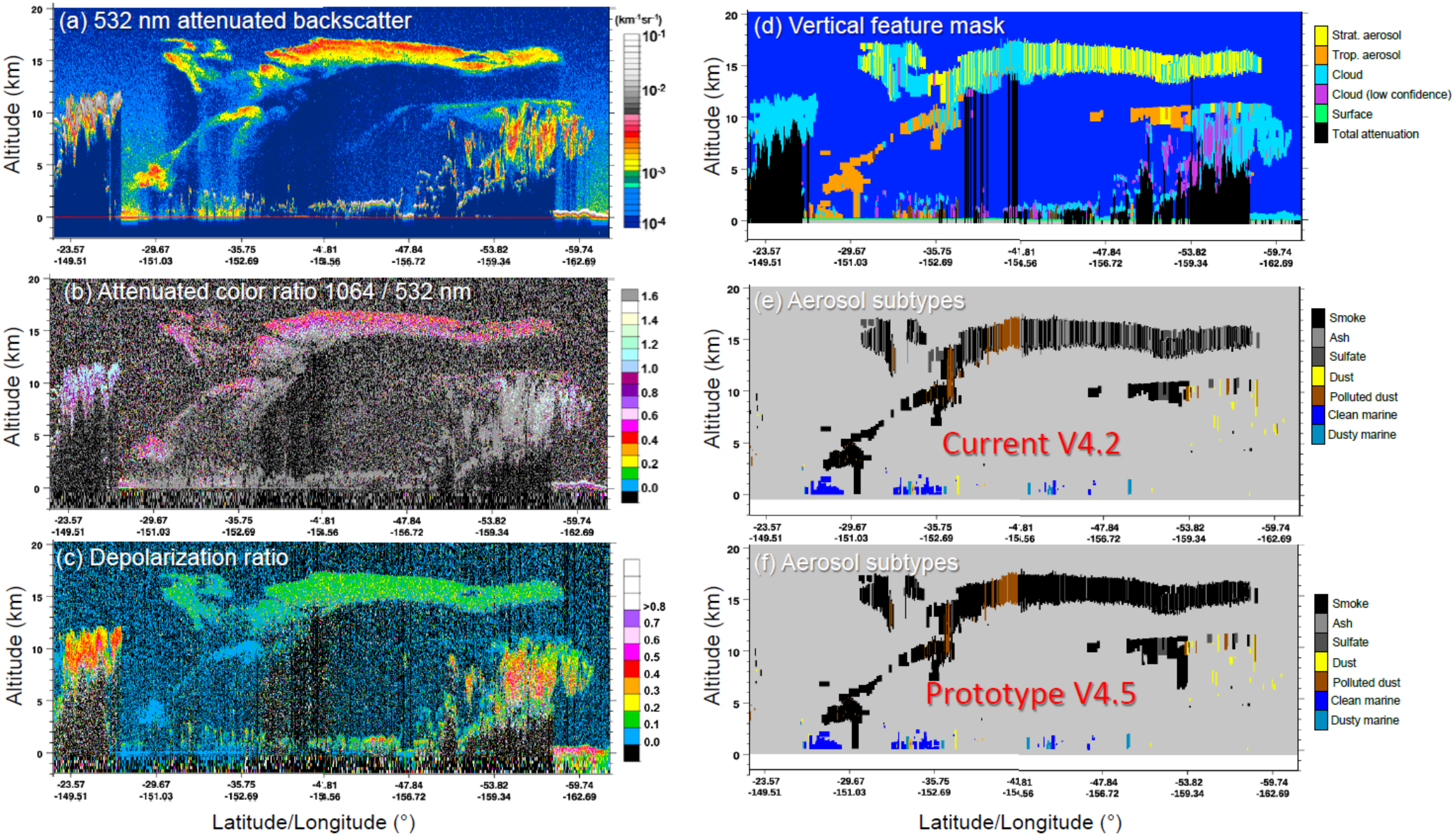

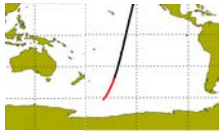

Aerosol Type Classification

The time series below show the rise in number of stratospheric aerosol layers detected by CALIOP in the southern hemisphere due to the Australian bushfires.The type classification is predominantly smoke (61%) for V4.5. Around 20% of the layers are misclassified as ash or sulfate. This is an improvement relative to the current V4.2 release which misclassifies 70% of these layers as ash or sulfate.

Daily CALIOP stratospheric aerosol classification below 20°S

Prototype V4.5

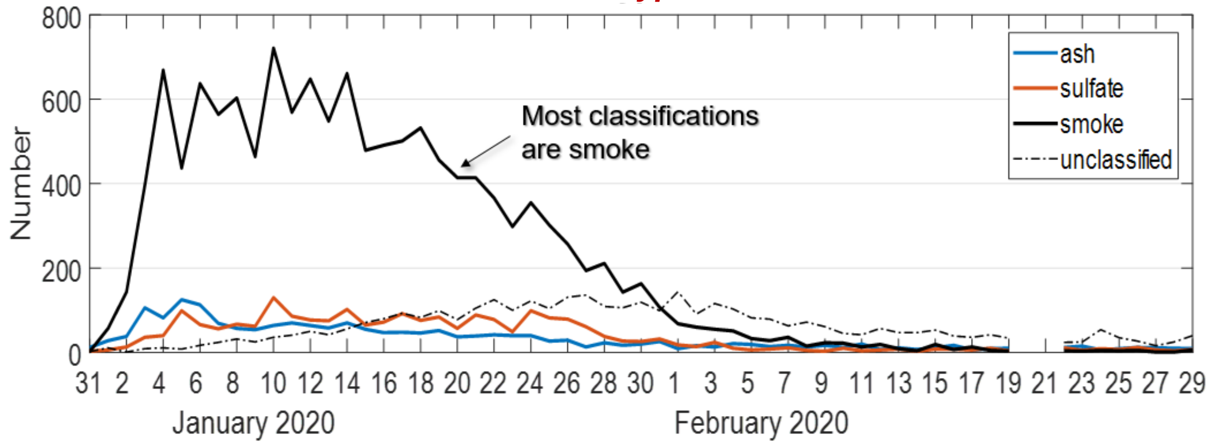

Current V4.2

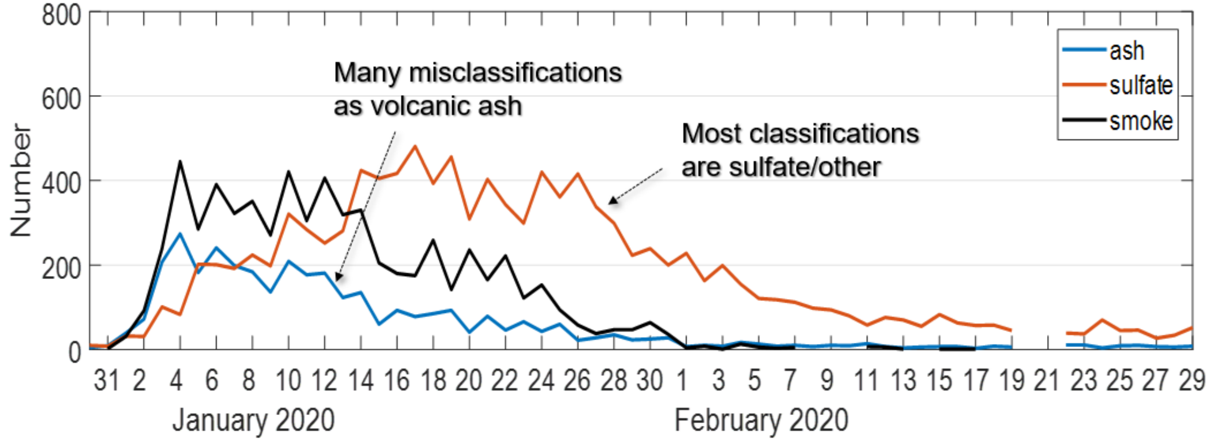

Upcoming Revisions to the Stratospheric Aerosol Typing Algorithm in V4.5

- Improved discrimination between depolarizing smoke and volcanic ash
- Improved discrimination between sulfate and weakly scattering stratospheric aerosol
- Increased opportunities for identifying ash, sulfate, and smoke among weakly scattering aerosol features

Distribution of Subtype Classification for All Stratospheric Aerosol Below 20°S; Dec 31, 2019 – Feb 29, 2020

	Upcoming V4.5	Current V4.2
Smoke	61.7 %	30.1 %
Ash	10.5 %	17.8 %
Sulfate	10.7 %	52.8 %
Unclassified	17.1 %	N/A

Mean Altitude of Stratospheric Smoke Layers

The maps show the mean top altitude of stratospheric layers identified as smoke by the prototype V4.5 aerosol typing algorithm following the pyroCb injections during December 2019/January 2020. A portion of the plume rose to very high altitudes (in red), reaching over 30 km in February. *Hatched areas are excluded to avoid low laser energy shots in the South Atlantic Anomaly region.*

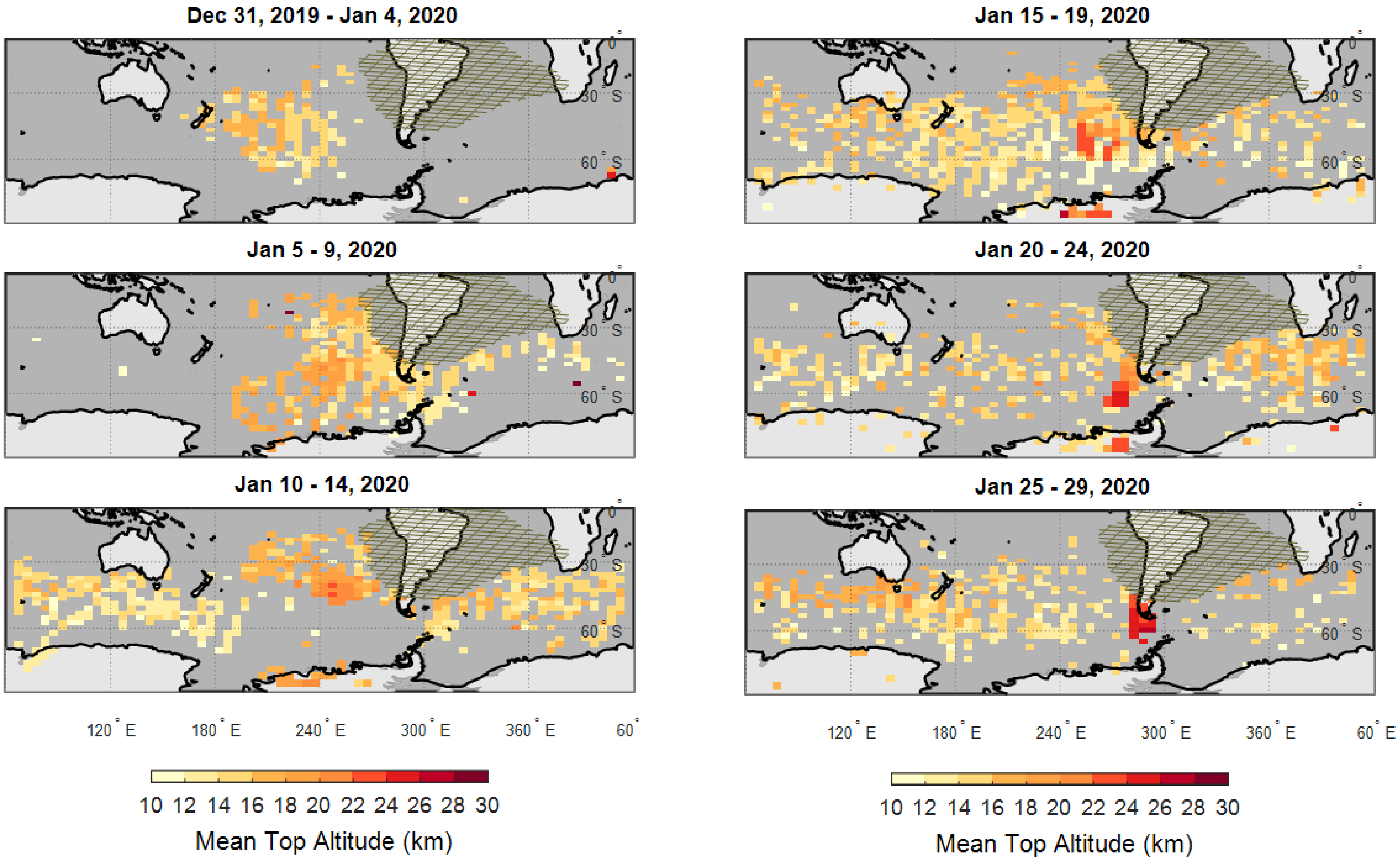

Measured Lidar Optical Properties of Smoke Comparison

The smoke plume reaching the stratosphere contained particles that were smaller and more aspherical compared to tropospheric smoke events. The 2D histograms below show the layer integrated attenuated color ratio (1064/532 nm attenuated backscatter) versus particulate depolarization ratio for tropospheric smoke events over North America and South Africa compared to stratospheric smoke from the Australian bushfire event. Color ratio increases with particle size and, for smoke, increases with layer optical depth. Particulate depolarization ratio is a proxy for asphericity.

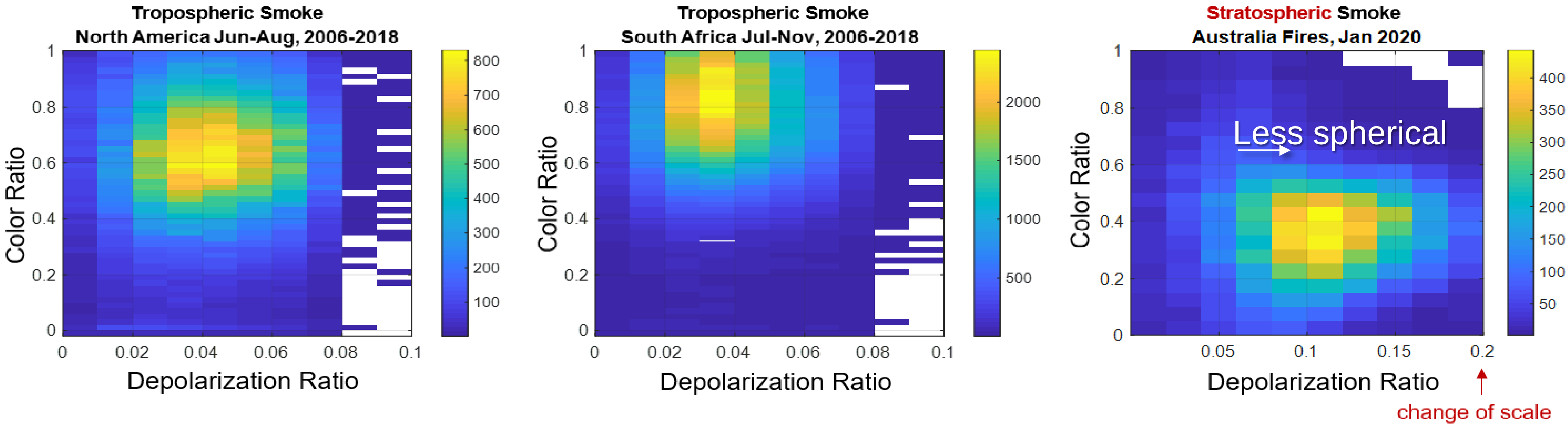

PMAp: synergistic aerosol products from Metop

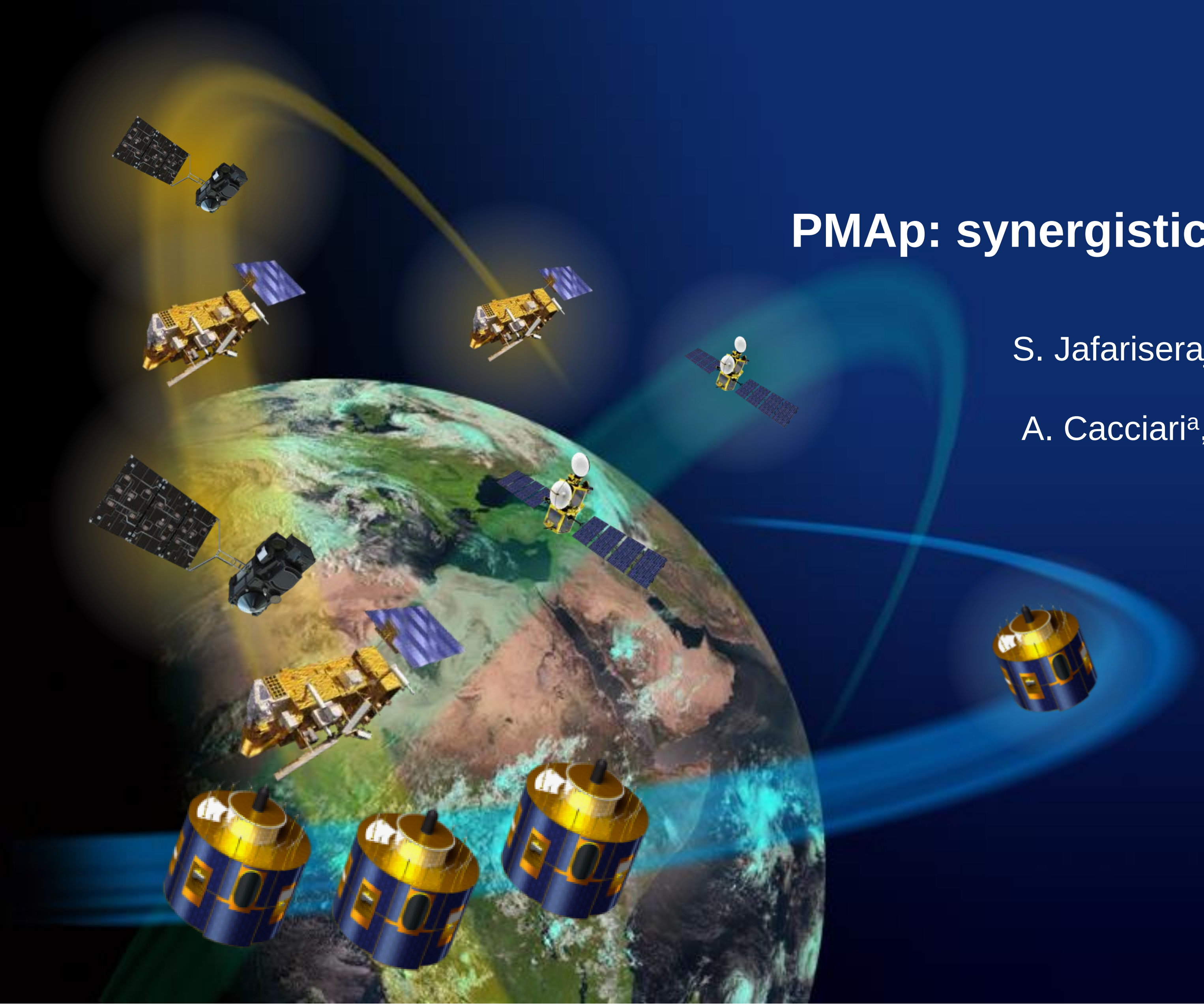

S. Jafariserajehlou[a,b], M. Vázquez-Navarro[a], A. Holdak[a,c],

A. Cacciari[a], B. Fougnie[a], G. Poli[a,d], R. Munro[a], R. Lang[a]

a EUMETSAT

b : Rhea Systems GmbH,

c: Vision Space Technologies,

d: IFAC-CNR

PMAp

The **Polar Multi-sensor Aerosol product (PMAp)**

is an operational aerosol product retrieved from **Metop A**, **B** and **C.**

PMAp AOD @550 nm, Metop (A+B+C)

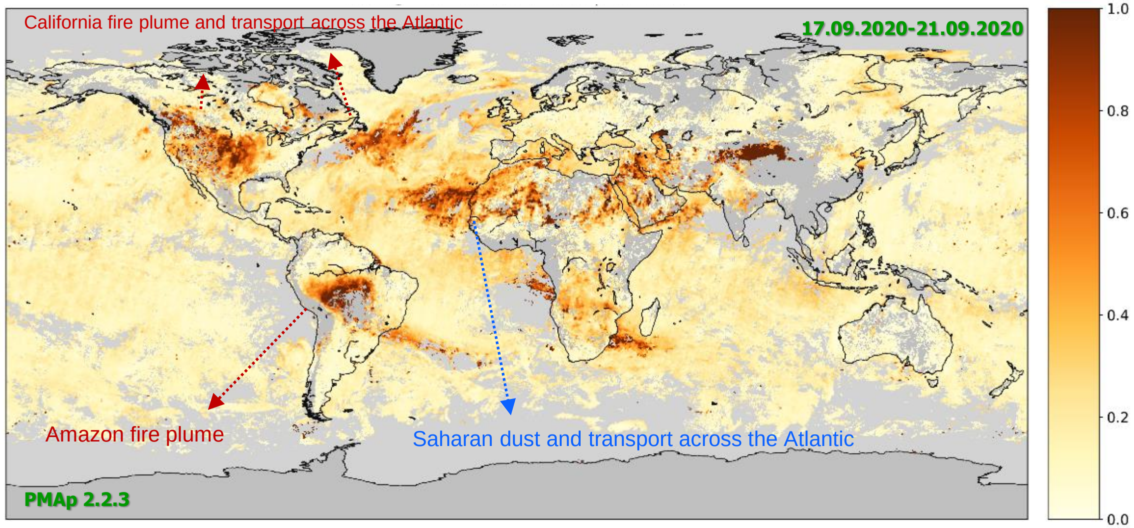

PMAp Aerosol Class, Metop (A+B+C)

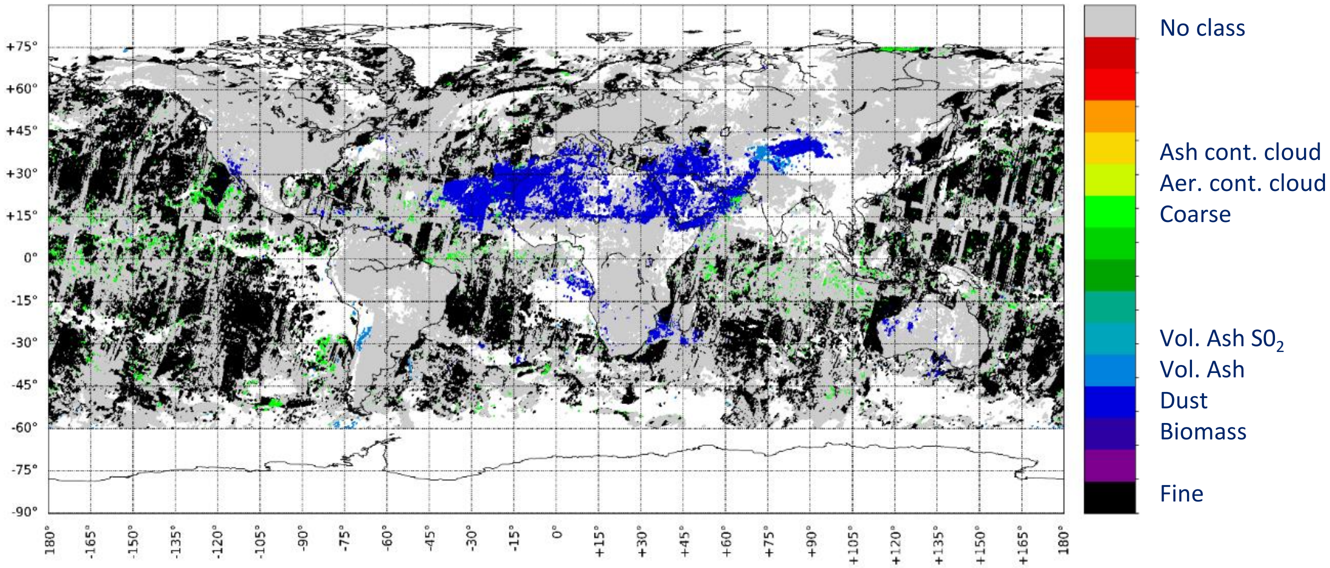

Near Real Time **Aerosol Optical Depth** and **Aerosol Type**

maximum 3 hours after sensing time, 24 hours a day

Assimilation start date: Ocean April 2014, Land: April, 2016.

Spatial coverage: Global, land and ocean

Spatial resolution: at GOME-2 PMD: Metop B and C: 10×40 km^2 ;Metop A: 5×40 km^2

Data availability:
- NRT product:
  Available via EUMETCast in netcdf4.

- Full orbit offline data.
  Available from the EUMETSAT archive
  http://archive.eumetsat.int EPS native and netcdf4.

PMAp: creating a hyper-instrument

Merging hyper-spectral and hyper-spatial information from GOME-2, AVHRR and IASI

Multi sensor spectral information

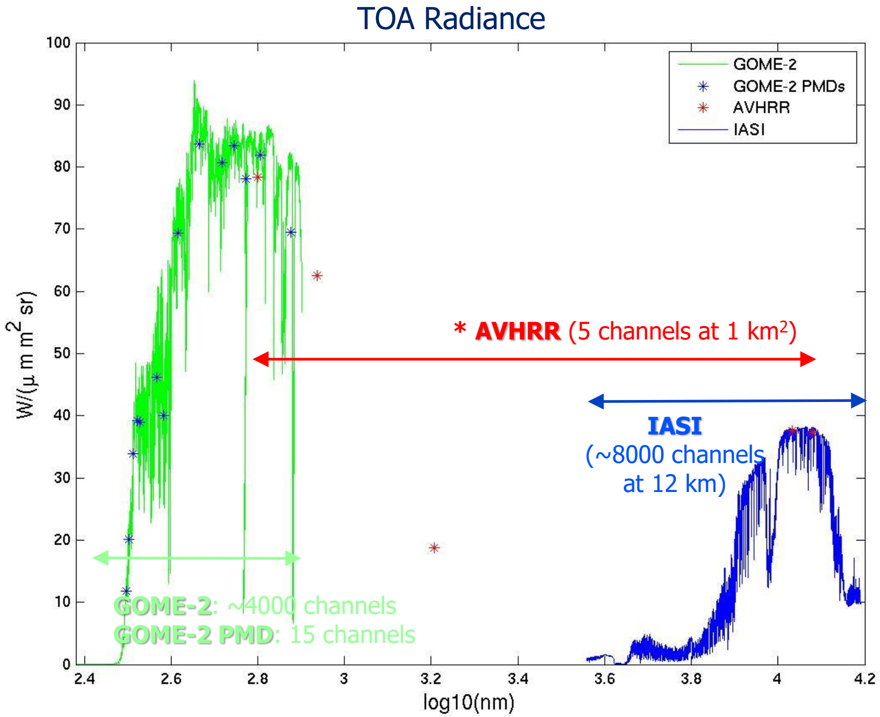

Multi sensor co-location

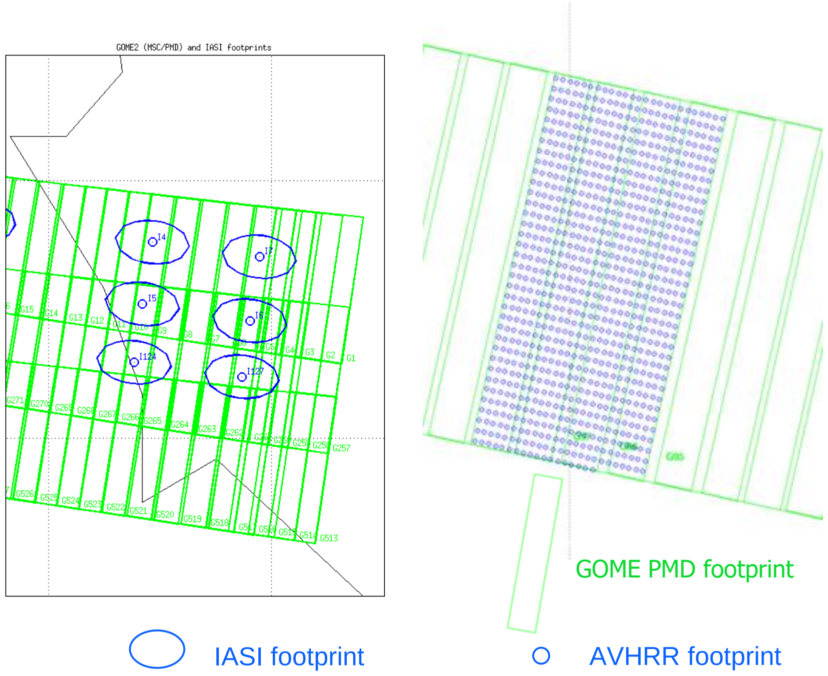

Instruments for L1 data	Spatial resolution	Spectral range	Purpose
GOME PMD	Metop B and C: 10×40 km^2 Metop A: 5×40 km^2	311 nm – 803 nm (15 band)	AOD, Aerosol Type, AAI, stokes fraction, polarization
AVHRR	1.08 × 1.08 km^2	580 nm – 12500 nm (5 band)	Clouds, scene heterogeneity, dust/ash
IASI	12 km (circular)	3700 nm – 15500 nm (resolution 0.5 cm^{-1})	Volcanic ash, desert dust, aerosol height

PMAp: algorithm description

PMAp retrieval algorithm design. Version 2.2.3 (next release):

Cloud/Aerosol discrimination

Cloud / Aerosol Discrimination

- **Volcanic Ash Detection**
  10 set of thresholds tests AVHRR + IASI BTDs tests → Ash presence
- **Desert Dust Detection**
  IASI dust index → Desert dust presence
- **Clouds' Detection & Correction**
  clouds detection and cloud fraction calculation (CF)
  cloud free PMD Reflectance .OR. PMD Reflectance Correction (for CF < 0.65; partly cloudy pixels)
- **Preliminary Aerosol Type**
  if Ash presence → aerosol type = ash
  if Dust presence → aerosol type = dust
  VIS/NIR test for Coarse/Fine mode determination
  } list of preselected aerosol types

Retrieve AODs

Retrieve AODs

- AODs retrieval for all aerosol models in the LUT
  over water PMD 12 (617.867 - 661.893 nm)
  over land PMD 8 (399.581 - 428.585 nm) or PMD 7 (380.186 - 383.753 nm)

Best fit selection {AOD, type}

best fit selection

- Microphysics fit : $\chi 2$ minimization of the AODs
  if cloud free: list of preselected aerosol types
  if partly cloud: all aerosol models
  } → best {AOD, aerosol type}
- Estimation of error on AOD

PMAp:

Version1 (water only)
Start of dissemination: 29th April 2014

Version 2.0 (water and land)
Start of dissemination: 17th April 2016

Version 2.1 (water and land)
Start of dissemination: 23rd February 2017

Version 2.2. (water and land)
Start of dissemination: Beginning 2021.

PMAp: comparison to MODIS

PMAp AOD @550 nm, Metop (A+B+C)

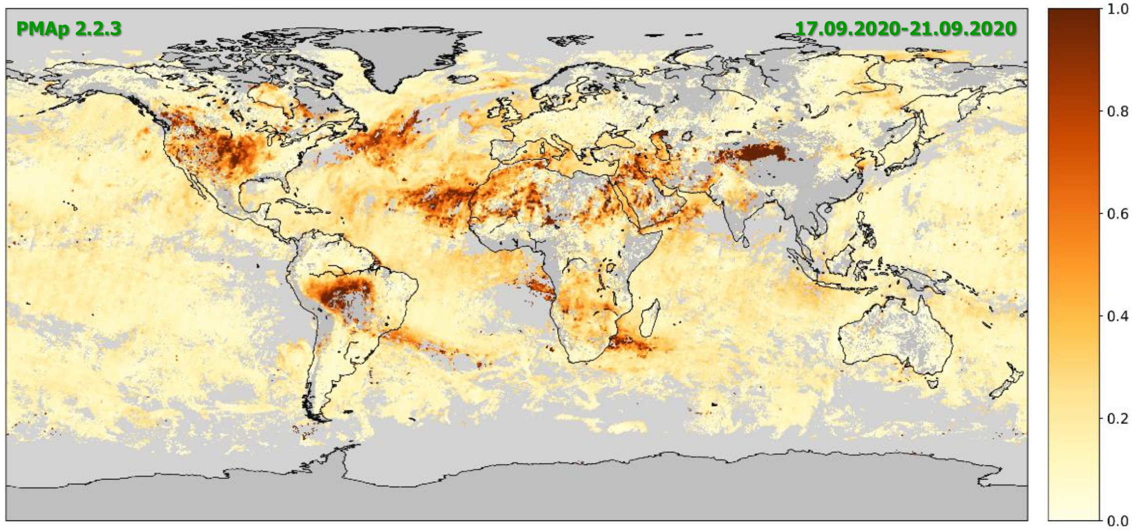

California fires, September 2020

PMAp

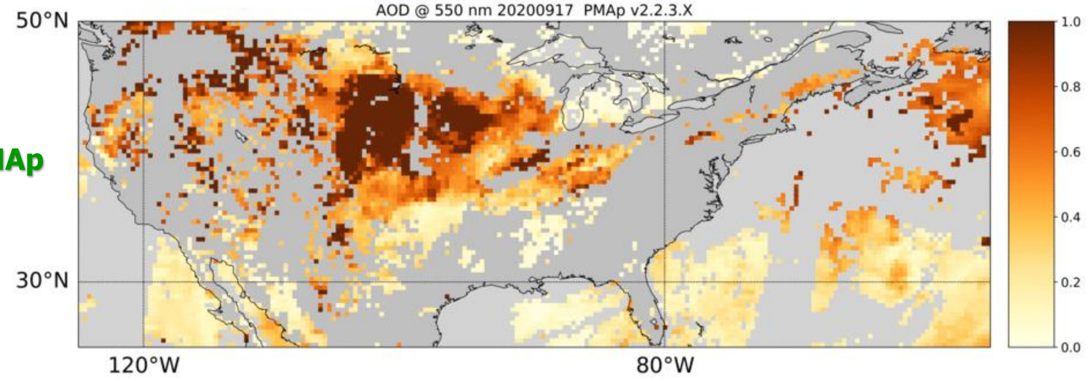

MODIS DT + DB

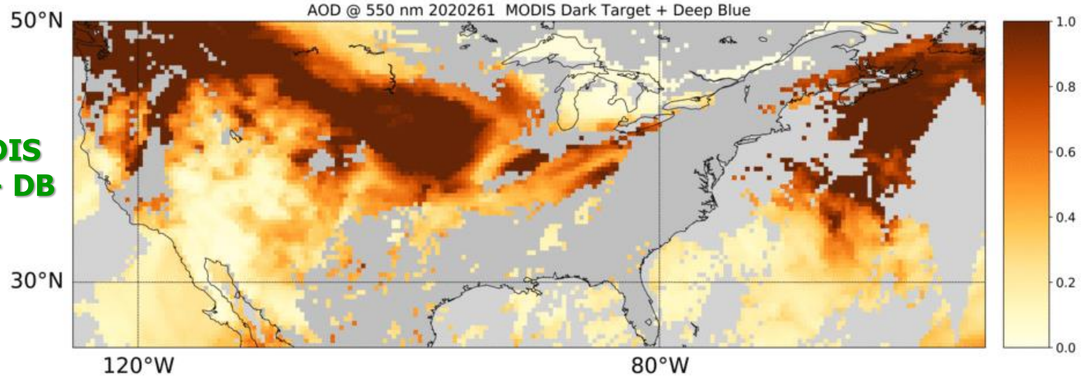

PMAp: comparison to SLSTR

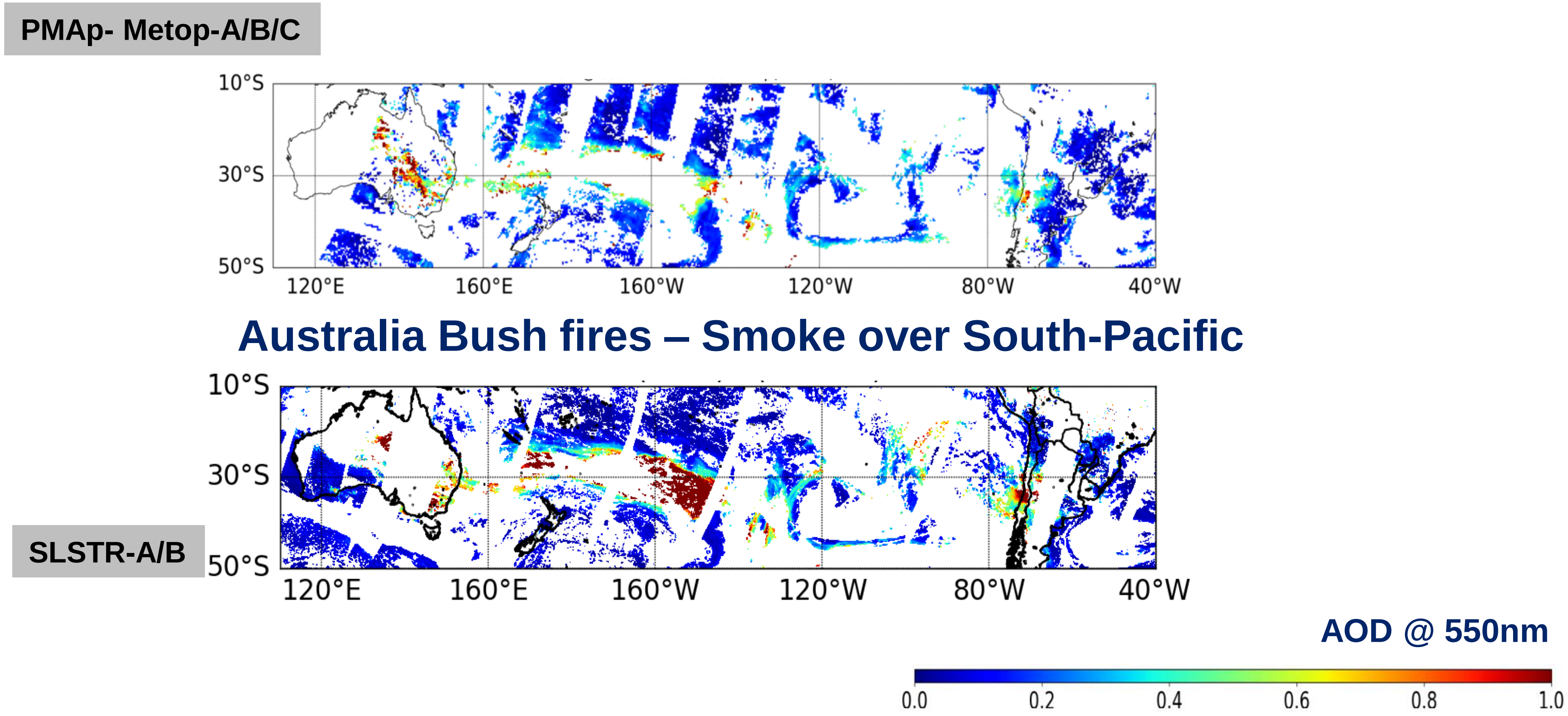

Model Enforced Post-Process Correction of Satellite Aerosol Retrievals

Antti Lipponen[1], Ville Kolehmainen[2], Pekka Kolmonen[1], Antti Kukkurainen[1], Tero Mielonen[1], Neus Sabater[1], Larisa Sogacheva[1], Timo H. Virtanen[1], and Antti Arola[1]
[1]Finnish Meteorological Institute, [2]University of Eastern Finland

- Idea is to take existing satellite retrievals and train a machine learning-based model to correct for the results given the retrievals and observations as inputs.

- Here we apply this method to MODIS Dark Target over land.

- AERONET is used as accurate aerosol data source when training the models and in validation

- We compare the post-process corrected AOD and AE, machine learning based AOD and AE, and the Dark Target AOD and AE with AERONET

- We see that post-process correction results in most accurate results

AMTD: https://doi.org/10.5194/amt-2020-229

Model Enforced Post-Process Correction of Satellite Aerosol Retrievals

Antti Lipponen[1], Ville Kolehmainen[2], Pekka Kolmonen[1], Antti Kukkurainen[1], Tero Mielonen[1], Neus Sabater[1], Larisa Sogacheva[1], Timo H. Virtanen[1], and Antti Arola[1]
[1]Finnish Meteorological Institute, [2]University of Eastern Finland

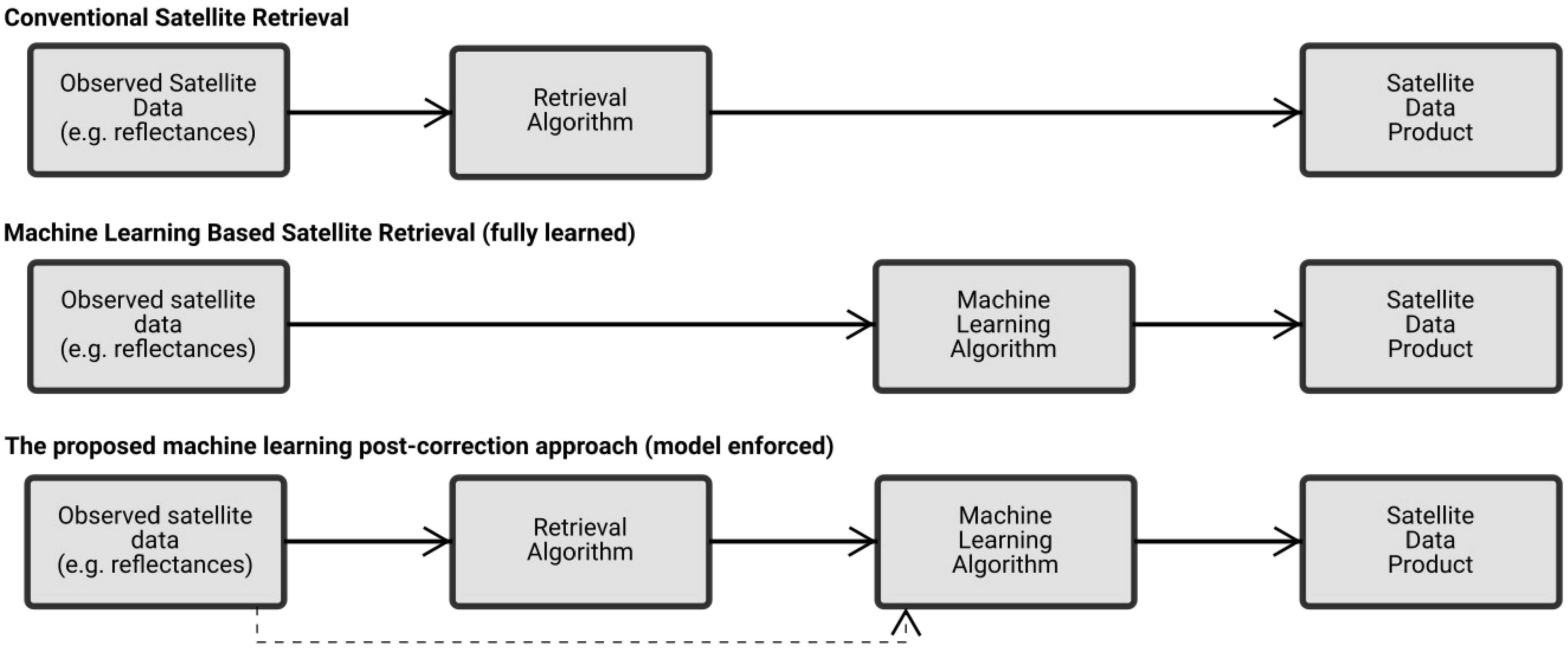

AMTD: https://doi.org/10.5194/amt-2020-229

Model Enforced Post-Process Correction of Satellite Aerosol Retrievals

Antti Lipponen[1], Ville Kolehmainen[2], Pekka Kolmonen[1], Antti Kukkurainen[1], Tero Mielonen[1], Neus Sabater[1], Larisa Sogacheva[1], Timo H. Virtanen[1], and Antti Arola[1]
[1]Finnish Meteorological Institute, [2]University of Eastern Finland

Our model:

Accurate retrieval algorithm (does not exist)

AOD
or
AE

Satellite observations (e.g. TOA reflectances, observation geometry etc.)

$$\begin{aligned} y &= f(\mathbf{x}) \\ &= \tilde{f}(\mathbf{x}) + \left[f(\mathbf{x}) - \tilde{f}(\mathbf{x})\right] \\ &= \tilde{f}(\mathbf{x}) + e(\mathbf{x}) \end{aligned}$$

Actual satellite retrieval algorithm (e.g. Dark Target)

Retrieval error

AMTD: https://doi.org/10.5194/amt-2020-229

Model Enforced Post-Process Correction of Satellite Aerosol Retrievals

Antti Lipponen[1], Ville Kolehmainen[2], Pekka Kolmonen[1], Antti Kukkurainen[1], Tero Mielonen[1], Neus Sabater[1], Larisa Sogacheva[1], Timo H. Virtanen[1], and Antti Arola[1]
[1]Finnish Meteorological Institute, [2]University of Eastern Finland

Our model:

Random Forest as regression model

	Regression	Correction
Inputs	Mean_TOA_Reflectance_0.47 Mean_TOA_Reflectance_0.55 Mean_TOA_Reflectance_0.65 Mean_TOA_Reflectance_0.86 Mean_TOA_Reflectance_1.24 Mean_TOA_Reflectance_1.63 Mean_TOA_Reflectance_2.11 STD_TOA_Reflectance_0.47 STD_TOA_Reflectance_0.55 STD_TOA_Reflectance_0.65 STD_TOA_Reflectance_0.86 STD_TOA_Reflectance_1.24 STD_TOA_Reflectance_1.63 STD_TOA_Reflectance_2.11 Scattering_Angle Sensor_Azimuth Sensor_Zenith Solar_Azimuth Solar_Zenith Topographic_Altitude_Land	AE (computed from Corrected_Optical_Depth_Lands) Surface_Reflectance_0.47 Surface_Reflectance_0.66 Surface_Reflectance_2.13 Corrected_Optical_Depth_Land_0.47 Corrected_Optical_Depth_Land_0.55 Corrected_Optical_Depth_Land_0.66 Land_Ocean_Quality_Flag Aerosol_Type_Land Mean_TOA_Reflectance_0.47 Mean_TOA_Reflectance_0.55 Mean_TOA_Reflectance_0.65 Mean_TOA_Reflectance_0.86 Mean_TOA_Reflectance_1.24 Mean_TOA_Reflectance_1.63 Mean_TOA_Reflectance_2.11 STD_TOA_Reflectance_0.47 STD_TOA_Reflectance_0.55 STD_TOA_Reflectance_0.65 STD_TOA_Reflectance_0.86 STD_TOA_Reflectance_1.24 STD_TOA_Reflectance_1.63 STD_TOA_Reflectance_2.11 Scattering_Angle Sensor_Azimuth Sensor_Zenith Solar_Azimuth Solar_Zenith Topographic_Altitude_Land
Outputs	AOD at 550 nm or AE (AERONET-based)	Additive correction *e* for AOD at 550 nm or AE (AERONET/MODIS -based)

AMTD: https://doi.org/10.5194/amt-2020-229

Model Enforced Post-Process Correction of Satellite Aerosol Retrievals

Antti Lipponen[1], Ville Kolehmainen[2], Pekka Kolmonen[1], Antti Kukkurainen[1], Tero Mielonen[1], Neus Sabater[1], Larisa Sogacheva[1], Timo H. Virtanen[1], and Antti Arola[1]
[1]Finnish Meteorological Institute, [2]University of Eastern Finland

AOD

AE

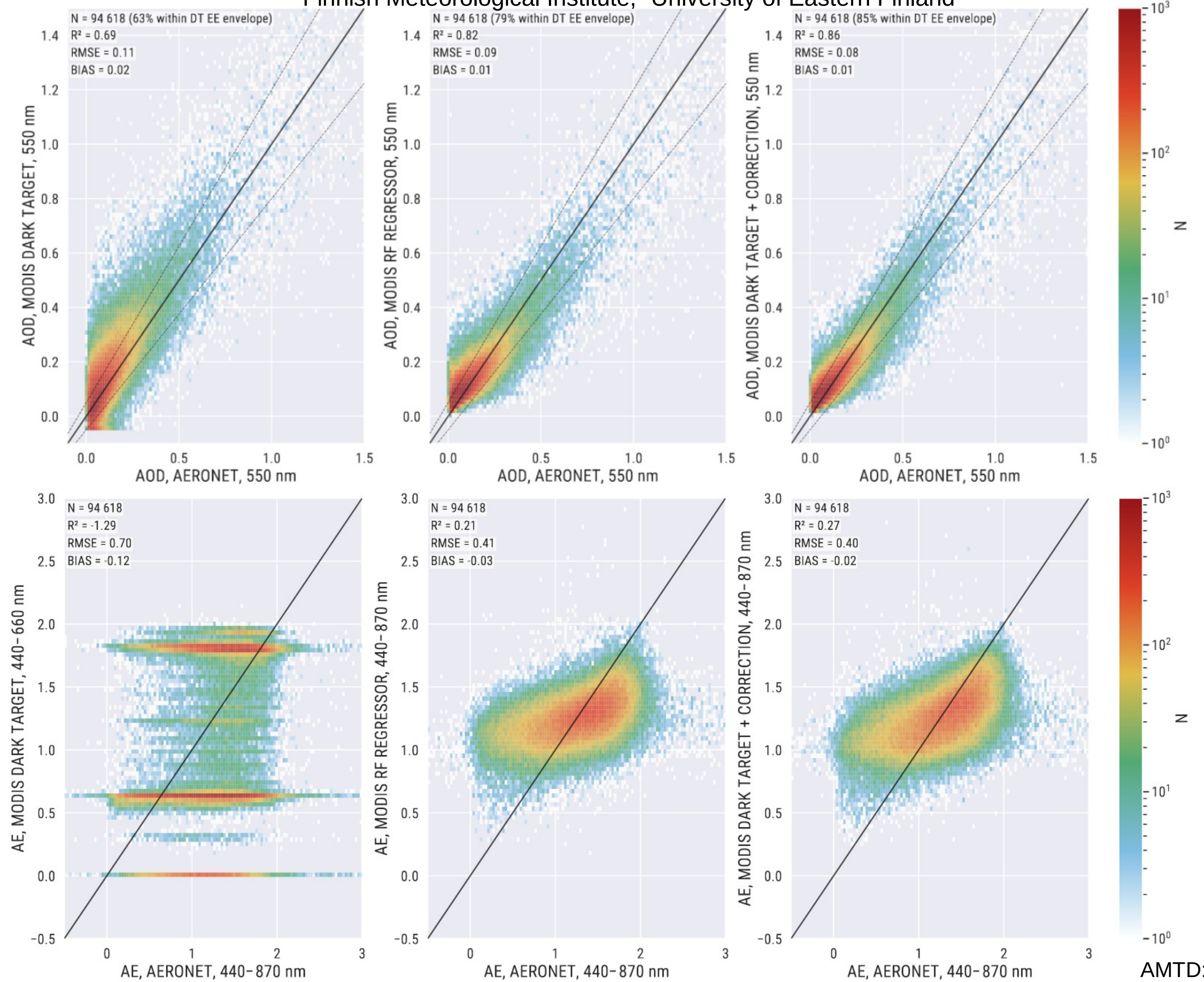

AMTD: https://doi.org/10.5194/amt-2020-229